Talazoparib and Niraparib

Subjects: Biochemistry & Molecular Biology

Contributor: Tina Jost

Niraparib (MK-4827) inhibits PARP1 and PARP2. It was approved by the U.S. Food and Drug Administration (FDA) in March 2017 indicated for the therapy of adult patients with ovarian, fallopian tube and peritoneal neoplasms. Talazoparib (BMN 673) is a potent and selective inhibitor of PARP1 and PARP2 used at lower concentrations than previous generations of PARP inhibitors. The FDA approved Talazoparib in October 2018 for patients with germline BRCA-mutated, HER2-negative breast cancer. Poly (ADP-ribose) polymerases (PARP) play an essential role in different cellular processes, including several pathways of DNA repair. PARP inhibitors (PARPi) are able to impair DNA damage repair by non-homologous end joining (NHEJ). This effect depends on the cell´s ability to compensate for the inhibition of PARP-mediated pathways by other repair pathways. PARPi especially induce cell death in cancer cells with a lack of PARP-independent DNA repair pathways.

Keywords: PARP ; kinase inhibitors ; ionizing radiation

1. Introduction

Niraparib (MK-4827) inhibits PARP1 and PARP2 [1]. It was approved by the U.S. Food and Drug Administration (FDA) in March 2017 indicated for the therapy of adult patients with ovarian, fallopian tube and peritoneal neoplasms [2]. Talazoparib (BMN 673) is a potent and selective inhibitor of PARP1 and PARP2 used at lower concentrations than previous generations of PARP inhibitors [3]. The FDA approved Talazoparib in October 2018 for patients with germline BRCA-mutated, HER2-negative breast cancer [4].

Poly (ADP-ribose) polymerases (PARP) play an essential role in different cellular processes, including several pathways of DNA repair [5][6][7]. PARP inhibitors (PARPi) are able to impair DNA damage repair by non-homologous end joining (NHEJ). This effect depends on the cell´s ability to compensate for the inhibition of PARP-mediated pathways by other repair pathways. PARPi especially induce cell death in cancer cells with a lack of PARP-independent DNA repair pathways. A known example of this synthetic lethality is the sensitivity of homologous recombinant (HR) deficient cells to PARPi [6][8]. Recently, this mechanism was confirmed in a clinical phase III trial using Olaparib in patients with homologous recombination deficient prostate cancers [9]. A further characteristic of PARPi is the so-called trapping of PARP. Trapped PARP does not dissociate from the lesion site and therefore blocks the damaged DNA position by complexation. This may reduce the possibility of completing DNA repair by other repair proteins [10]. Consequently, repair incompetence and accumulation of DNA lesions cause increased genomic instability and a higher probability of cell death [5][6].

Furthermore, PARPi treatment could be extended to cancer treatment in combination with DNA-damaging treatments [10]. The principle of enhancing the DNA-damaging effect of radiotherapy with simultaneous chemotherapy is widely known [11]. It has been suggested that PARPi offer the opportunity to enhance the efficacy of radiotherapy [7][12]. Noticeably, some DNA damage repair protein inhibitors targeting double-strand break repair proteins are also known to influence radiation therapy on a cellular level [13]. However, an increased risk of side effects after simultaneous therapy with kinase inhibitors and irradiation is described [14][15]. Based on commonly used melanoma cell lines Weigert/Jost et al. [16] have done a first overview study about the influence of the two PARPi Niraparib and Talazoparib in combination with ionizing radiation on melanoma cell cultures in vitro.

2. PARP1 and PARP2 levels in different cell lines

The baseline PARP1 and PARP2 levels were higher in the four melanoma cell lines ANST, ARPA, RERO and LIWE compared to the two healthy skin fibroblast cell cultures SBLF7 and SBLF9 (Figure 1A). In the control groups of the four melanoma cell lines, ANST, ARPA, RERO and LIWE, the relative levels of PARP1 appeared to be higher than those of PARP2. The untreated control groups of the LIWE, RERO and ARPA cell lines tended to have a higher PARP1 level than the ANST cell line. Combined treatment of Talazoparib plus IR tended to decrease PARP1 in ARPA, RERO and LIWE cancer cell cultures. Similarly, after the application of Niraparib plus IR, the PARP1 level tended to decrease in the RERO

and LIWE cell cultures. Contrary to that, in the ARPA cell culture, the PARP1 content seemed to increase after the combined treatment of Niraparib plus IR. ANST cell line did not change their PARP1 levels after treatment with inhibitor and IR. The PARP2 expression in the untreated control groups of all four tested melanoma cell cultures indicated similar levels. A combined treatment of these melanoma cell cultures with Talazoparib respectively Niraparib plus IR tended to increase the PARP2 content (Figure 1B,C). Furthermore, data were then normalized to β-Actin to avoid possible bias of different GAPDH expression which is known for different cancer cells. To summarize, a combined treatment of PARP inhibitor and IR primarily resulted in a decrease or a constant level of PARP1 content, whereas the PARP2 content increased in all four melanoma cell lines. No statistical significance could be derived from our experiments, but nevertheless, interesting tendencies emerged.

3. Induction of Apoptosis and Necrosis by PARPi

Two characteristic examples of the Kaluza analysis of our apoptosis and necrosis experiments are displayed (Figure 2A,B). Most of the cells were neither Annexin nor 7-AAD positive and therefore identified as living cells. This cluster of living cells is depicted in the lower-left quadrant of the chart. After combined treatment with PARP inhibitor plus IR, the cells slightly increased in the lower right Annexin-positive quadrant, representing apoptosis. The Annexin plus 7-AAD-positive upper right quadrant represents necrosis (Figure 2B). The combined treatment is compared to the untreated controls (Figure 2A).

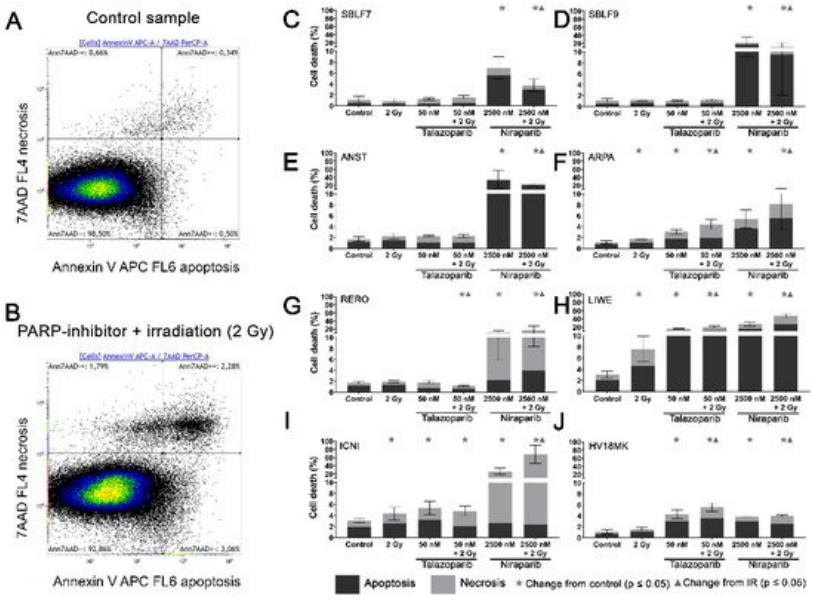

Figure 2. Apoptotic and necrotic rates after combined PARPi plus IR treatment. Healthy skin fibroblast and melanoma cell cultures were analyzed 48 h after the treatment with IR, with a PARPi Talazoparib (50 nM) respectively Niraparib (2500 nM), with IR plus an inhibitor or without treatment with regard to their apoptotic and necrotic rates. (**A**) Control sample and (**B**) a sample after combined treatment of PARPi plus IR in the flow cytometer analysis of Annexin/7-AAD staining. (**C–J**) Apoptotic and necrotic rates in eight different cell cultures. A logarithmic scaling was chosen for a better representability. The data were analyzed using the Mann–Whitney-U test.

In the subsequent analysis, apoptosis and necrosis are summarized as cell death. In the healthy fibroblast cell lines SBLF7 respectively SBLF9 (Figure 2C,D), neither the IR treatment nor the Talazoparib mono-treatment nor the combined treatment of Talazoparib plus IR led to a significant change in the cell death rate compared to the control groups. However, in both fibroblast cell cultures, the Niraparib treatment significantly increased cell death. Likewise, the combined treatment of Niraparib plus IR increased cell death ($p = 0.036$ respectively $p = 0.048$). In the cancer cell lines (Figure 2E–J), the rates of cell death induction varied distinctly more than in the healthy fibroblasts. After IR treatment, cell death increased clearly in ARPA, LIWE and ICNI melanoma cell lines ($p \leq 0.05$) (Figure 2F,H,I). The IR treatment did not noticeably induce cell death in ANST, RERO and HV18MK melanoma cell lines (Figure 2E,G,J). Talazoparib treatment did increase the rate of cell death in ARPA, ICNI, HV18MK and most in LIWE cell lines ($p \leq 0.05$) (Figure 2F,I,J,H). After a combined treatment of Talazoparib plus IR, the cell death increased between 2% and 18% in ICNI, ARPA, HV18MK and again most in LIWE ($p \leq 0.05$) (Figure 2I,F,J,H). Furthermore, a significant increase in cell death compared to the IR mono-treatment was observable in ARPA, HV18MK and LIWE, varying between 3% and 13% ($p \leq 0.05$). After combined Talazoparib plus IR treatment, however, cell death decreased slightly in the RERO cell culture compared to the untreated control group as well as to the IR mono-treatment (Figure 2G). In all melanoma cell cultures, the Niraparib treatment and the combined treatment of Niraparib plus IR again led to an increase in cell death. This increase was 3% in HV18MK as

well as 65% in ICNI. The increases in the other four melanoma cell lines were scattered between these two values ($p \leq 0.05$). In addition, the combined treatment of Niraparib plus IR increased cell death compared to the IR mono-treatment, varying between a 2% increase in HV18MK and a 64% increase ICNI ($p \leq 0.05$).

The difference between the sum of the particular mono-treatments and the corresponding combined treatment was calculated to obtain PARPi and IR interactions. The underlying values of the logarithmic graphs in Figure 2C–J were used. Sub-additive effects were observed in the SBLF9 and the ANST cell lines after the combined treatment of Niraparib plus IR (SBLF9: −10%; ANST: −12%). In contrast, supra-additive effects were observed in the LIWE and the ICNI cell lines after the combination of Niraparib plus IR (LIWE: +12%; ICNI: +38%). For the remaining cell lines, the effects were approximately additive.

4. Cell Cycle G2/M Arrest

Cell cycle arrest in the G2/mitosis (G2/M) phase was studied using Hoechst 33342 DNA staining. The DNA content was graphically visualized (Figure 3A,B). The first peak represents the G0/G1 phase cells with single DNA content and the second peak represents the G2/M phase cells with double DNA content. The S phase cells are in between the two peaks (Figure 3A). A combined treatment leads to an increase in the G2/M phase (Figure 3B).

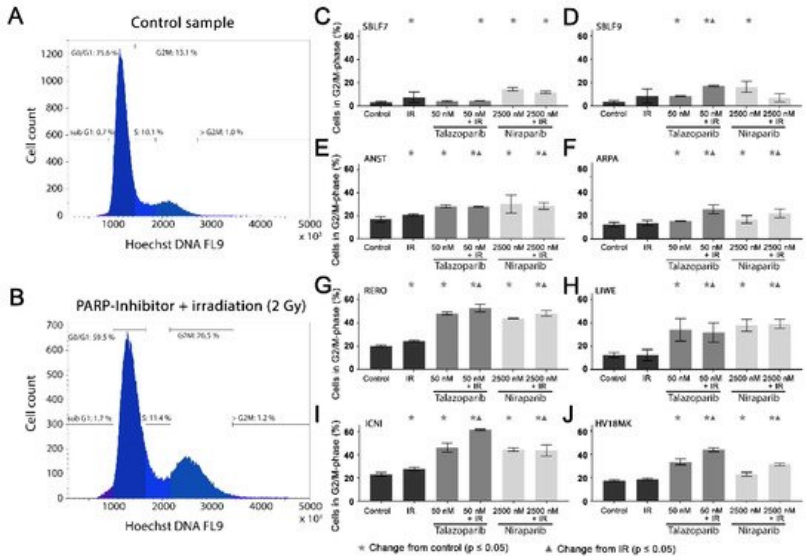

Figure 3. G2/M phase arrest after combined PARPi plus IR treatment. The G2/M phase content of healthy skin fibroblast and melanoma cell cultures. The DNA content was analyzed by flow cytometry of Hoechst 33342 staining 48 h after the treatment with IR, with a PARPi (50 nM Talazoparib respectively 2500 nM Niraparib) or with IR plus an inhibitor. The control groups stayed untreated. (**A**) Histogram of the cells in the different cell cycle phases of a control sample. (**B**) A sample after a combined treatment of PARPi plus IR. (**C–J**) G2/M phase fraction in eight different cell cultures. The data were analyzed using the Mann–Whitney-U test.

In the healthy fibroblasts SBLF7 and SBLF9, the G2/M phase cells accounted for 3% (Figure 3C,D). IR treatment increased the G2/M cell cycle arrest of the fibroblasts. After the combined treatment of Talazoparib plus IR, the G2/M fraction of the two healthy fibroblast cell lines did increase ($p \leq 0.05$). Niraparib mono-treatment did increase the G2/M fraction, whereas the combined treatment tended to reduce this effect.

The G2/M levels in the melanoma cell lines (Figure 3E–J) were distinctly higher than in the fibroblasts, varying between 12% in the ARPA and 23% in the ICNI cell cultures. In the treated groups, G2/M arrest increased in the melanoma cell cultures more than in the fibroblast cultures. IR treatment did increase the G2/M fraction in the ANST, RERO and ICNI cultures (Figure 3E,G,I). After treatment with one of the inhibitors as well as after combined treatment with one inhibitor plus IR, the arrest in G2/M did increase in all melanoma cell cultures: 3% in ARPA up to 38% in ICNI, with the values of the other four melanoma cell lines scattering in between ($p \leq 0.05$). Compared to the IR mono-treatment, the combined treatment with one inhibitor plus IR did increase the G2/M arrest values in all melanoma cell cultures, varying between 7% in ANST and 34% in ICNI ($p \leq 0.05$). There are large differences in G2/M arrest between the different cell lines. Additionally, we analyzed the subG1 phase for comparison with our cell death FACS analysis.

5. Surviving Fraction

Cell surviving was observed for the two healthy fibroblasts and for five melanoma cell lines by the colony formation assay. Images of Petri dishes from a control sample and after treatment are shown (Figure 4A). The healthy fibroblast cultures SBLF7 and SBLF9 (Figure 4B,C) were clearly sensitive against the inhibitors themselves and even more against the combined treatment of an inhibitor plus IR. The melanoma cell lines ARPA, RERO and LIWE were similarly sensitive (Figure 4E–G). The HV18MK melanoma cell culture was apparently less sensitive against the combined treatment and not sensitive against the inhibitors (Figure 4H). The ANST melanoma cell culture was neither sensitive against the inhibitors nor the combined treatment (Figure 4D).

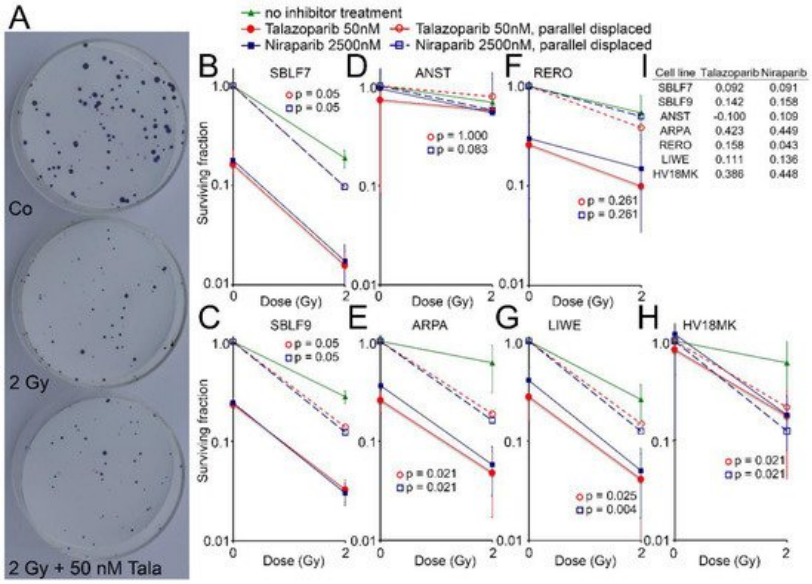

Figure 4. Colony formation assay after combined PARPi plus IR treatment. (**A**) Representativ colony formation assay in petri dishes of skin cancer cell line RERO untreated (Co), irradiated (2 Gy) and after combined therapy (2 Gy + 50 nM Talazoparib). (**B–H**) Surviving fraction after 0 and 2 Gy IR and after treatment with the PARPi Talazoparib (50 nM, red lines) respectively Niraparib (2500 nM, blue lines) (Solid lines). Normalized values for the effect of the inhibitors (stripped lines). (**I**) The difference between the parallel displaced values of the combined effect and the radiation effect alone indicating the increased effect of the combined treatment.

The curves of the combined treated cell lines were shifted parallel to display the interaction between the inhibitors and irradiation. The differences of the parallel displaced combined treatment to IR treatment alone are listed in Figure 4I, representing a deviation from a supposed additive effect. In the cell lines ARPA and HV18MK, a pronounced supra-additive effect was observed for both inhibitors ($p \leq 0.05$). For the fibroblasts and the melanoma cell cultures ANST, RERO and LIWE, there were minor supra-additive effects and in the case of ANST, there were none for Talazoparib.

6. Homologous Recombination Status

Additionally, we analyzed the homologous recombination (HR) status of the cell lines. The healthy fibroblasts SBLF7 and SBLF9 as well as the melanoma cell lines ANST and LIWE were HR-proficient, which was indicated by an increase of the RAD51 foci. RAD51 foci decreased in the melanoma cell cultures ARPA, RERO, ICNI and HV18MK and therefore these cell lines were defined as HR-deficient.

7. Conclusion and outlook

We found that most of the melanoma cell lines studied were sensitive to the combined treatment with inhibitors and irradiation with regard to cell survival: four out of six cell lines were sensitive to Talazoparib plus IR treatment and six out of six cell lines were sensitive to Niraparib plus IR treatment. These results were even more pronounced when considering clonogenic survival: four out of five cell lines were sensitive to both inhibitors in combination with irradiation treatment. In addition, we found a clear potential for radiosensitization of melanoma cells with both inhibitors in combination with irradiation: in six out of six cell lines, the proportion of cells in the G2/M phase increased. This radiosensitization could increase the efficiency in clinical radiotherapy of melanoma patients. In addition, the less radiation-sensitive healthy tissue would be spared during therapy. However, we could not establish a general benefit of the combined therapy, since individual melanoma cell lines are resistant to the therapy. Therefore, an individualization of the therapy with prior testing of the tumor tissue should be the first step towards efficient combination therapy.

References

1. National Center for Biotechnology Information-Compound Summary Niraparib . National Center for Biotechnology Information-Compound Summary Niraparib. Retrieved 2021-6-24
2. FDA-Niraparib (Zejula) . FDA-Niraparib (Zejula). Retrieved 2021-6-24
3. Johann De Bono; Ramesh K. Ramanathan; Lida Mina; Rashmi Chugh; John Glaspy; Saeed Rafii; Stan Kaye; Jasgit Sachdev; John Heymach; David C. Smith; et al. Phase I, Dose-Escalation, Two-Part Trial of the PARP Inhibitor Talazoparib in Patients with Advanced Germline BRCA1/2 Mutations and Selected Sporadic Cancers. *Cancer Discovery* **2017**, *7*, 620-629, 10.1158/2159-8290.cd-16-1250.
4. FDA Approves Talazoparib for gBRCAm HER2-Negative Locally Advanced or Metastatic Breast Cancer . FDA Approves Talazoparib for gBRCAm HER2-Negative Locally Advanced or Metastatic Breast Cancer. Retrieved 2021-6-24
5. Julio C. Morales; Longshan Li; Farjana J. Fattah; Ying Dong; Erik A. Bey; Malina Patel; Jinming Gao; David A. Boothman; Review of Poly (ADP-ribose) Polymerase (PARP) Mechanisms of Action and Rationale for Targeting in Cancer and Other Diseases. *Critical Reviews in Eukaryotic Gene Expression* **2014**, *24*, 15-28, 10.1615/critreveukaryotgeneexpr.2013006875.
6. Jac A. Nickoloff; Dennie Jones; Suk-Hee Lee; Elizabeth A. Williamson; Robert Hromas; Drugging the Cancers Addicted to DNA Repair. *Journal of the National Cancer Institute* **2017**, *109*, 109, 10.1093/jnci/djx059.
7. Paul Lesueur; François Chevalier; Jean-Baptiste Austry; Waisse Waissi; Hélène Burckel; Georges Noel; Jean-Louis Habrand; Yannick Saintigny; Florence Joly; Poly-(ADP-ribose)-polymerase inhibitors as radiosensitizers: a systematic review of pre-clinical and clinical human studies. *Oncotarget* **2017**, *8*, 69105-69124, 10.18632/oncotarget.19079.
8. Nuala McCabe; Nicholas C. Turner; Christopher Lord; Katarzyna Kluzek; Aneta Białkowska; Sally Swift; Sabrina Giavara; Mark J. O'connor; Andrew N. Tutt; Małgorzata Z. Zdzienicka; et al. Deficiency in the Repair of DNA Damage by Homologous Recombination and Sensitivity to Poly(ADP-Ribose) Polymerase Inhibition. *Cancer Research* **2006**, *66*, 8109-8115, 10.1158/0008-5472.can-06-0140.
9. De Bono, Mateo, Flzazi, Saad, Shore, Sandhu, Chi, Sartor, Agarwal, Olmos; Olaparib for Metastatic Castration-Resistant Prostate Cancer. *New England Journal of Medicine* **2020**, *383*, 890-891, 10.1056/nejmc2023199.
10. Valeria Ossovskaya; Ingrid Chou Koo; Eric P. Kaldjian; Christopher Alvares; Barry M. Sherman; Upregulation of Poly (ADP-Ribose) Polymerase-1 (PARP1) in Triple-Negative Breast Cancer and Other Primary Human Tumor Types. *Genes & Cancer* **2010**, *1*, 812-821, 10.1177/1947601910383418.
11. Yvonne Lorat; Jochen Fleckenstein; Patric Görlinger; Christian Rübe; Claudia E. Rübe; Assessment of DNA damage by 53PB1 and pKu70 detection in peripheral blood lymphocytes by immunofluorescence and high-resolution transmission electron microscopy. *Strahlentherapie und Onkologie* **2020**, *196*, 821-833, 10.1007/s00066-020-01576-1.
12. Joaquin Mateo; C.J. Lord; Violeta Serra; A. Tutt; Judith Balmaña; M. Castroviejo-Bermejo; C. Cruz; Ana Oaknin; S.B. Kaye; J.S. de Bono; et al. A decade of clinical development of PARP inhibitors in perspective. *Annals of Oncology* **2019**, *30*, 1437-1447, 10.1093/annonc/mdz192.
13. Felix Bürkel; Tina Jost; Markus Hecht; Lucie Heinzerling; Rainer Fietkau; Luitpold Distel; Dual mTOR/DNA-PK Inhibitor CC-115 Induces Cell Death in Melanoma Cells and Has Radiosensitizing Potential. *International Journal of Molecular Sciences* **2020**, *21*, 9321, 10.3390/ijms21239321.
14. M. Hecht; L. Zimmer; C. Loquai; C. Weishaupt; R. Gutzmer; B. Schuster; S. Gleisner; B. Schulze; S. M. Goldinger; C. Berking; et al. Radiosensitization by BRAF inhibitor therapy—mechanism and frequency of toxicity in melanoma patients. *Annals of Oncology* **2015**, *26*, 1238-1244, 10.1093/annonc/mdv139.
15. Thomas Gryc; Florian Putz; Nicole Goerig; Sonia Ziegler; Rainer Fietkau; Luitpold V. Distel; Barbara Schuster; Idelalisib may have the potential to increase radiotherapy side effects.. *Radiation Oncology* **2017**, *12*, 109, 10.1186/s13014-017-0827-7.
16. Verena Weigert; Tina Jost; Markus Hecht; Ilka Knippertz; Lucie Heinzerling; Rainer Fietkau; Luitpold V. Distel; PARP inhibitors combined with ionizing radiation induce different effects in melanoma cells and healthy fibroblasts. *BMC Cancer* **2020**, *20*, 1-10, 10.1186/s12885-020-07190-9.